Energy & Environmental Science

Cite this: *Energy Environ. Sci.*, 2012, **5**, 6885

www.rsc.org/ees

COMMUNICATION

Rhodium–nickel nanoparticles grown on graphene as highly efficient catalyst for complete decomposition of hydrous hydrazine at room temperature for chemical hydrogen storage†

Jun Wang, Xin-Bo Zhang,* Zhong-Li Wang, Li-Min Wang and Yu Zhang*

Received 1st December 2011, Accepted 22nd February 2012
DOI: 10.1039/c2ee03344e

Well-dispersed rhodium–nickel nanoparticles grown on graphene are successfully synthesized by co-reduction of graphene oxide and metal precursors, wherein graphene proved to be a powerful dispersion agent and distinct support for the RhNi nanoparticles. Unexpectedly, the resultant RhNi@graphene catalyst exerts 100% selectively and exceedingly high activity to complete the decomposition reaction of hydrous hydrazine at room temperature. This excellent catalytic performance might be due to the synergistic effect of the graphene support and the RhNi nanoparticles and the promotion effect of NaOH. The utilization of graphene as a novel two-dimensional catalyst support to anchor active component nanoparticles and thus to facilitate the electron transfer and mass transport kinetics during the catalytic reaction process opens up new avenues for designing next-generation catalysts.

State Key Laboratory of Rare Earth Resource Utilization, Changchun Institute of Applied Chemistry (CIAC), Chinese Academy of Sciences (CAS), 130022 Changchun, China. E-mail: xbzhang@ciac.jl.cn; zhangyu@ciac.jl.cn.

† Electronic supplementary information (ESI) available: Synthesis conditions; experimental procedures; ICP-AES, SEM and TEM analyses of the nanoparticles; UV-Vis tests of the solution before and after reaction; hydrous hydrazine decomposition reaction results under different conditions. See DOI: 10.1039/c2ee03344e

The search for effective hydrogen-storage materials remains one of the most challenging barriers in the implementation of a "hydrogen economy" society, even after several decades of intensive exploration.[1] Its solution requires innovative breakthroughs coming from scientific and technological research that looks beyond the storage materials currently known.[1,2] Hydrazine monohydrate ($H_2NNH_2 \cdot H_2O$) is considered as a promising hydrogen storage material because of its high hydrogen content (8.0 wt%),[3,4] easy recharging as a liquid, and production of only nitrogen in addition to hydrogen *via* a complete decomposition reaction: $H_2NNH_2 \rightarrow N_2(g) + 2H_2(g)$. However, to maximize the efficacy of hydrazine as a hydrogen storage material, one must avoid the undesired reaction pathway: $3H_2NNH_2 \rightarrow 4NH_3 + N_2(g)$.[3] Although 100% catalytic selectivity has already been successfully achieved, the catalytic kinetics is still terribly sluggish[4] which greatly hinders the practical application of this system. Therefore, the development of highly selective and highly efficient catalyst to significantly improve the kinetic properties for the catalytic decomposition of hydrous hydrazine at room temperature is urgently important for its practical application.

Nanocatalysis has been contributing significantly to many important chemical reactions due to its large surface-to-volume ratio and the enhanced surface atomic catalytic activity compared to its bulk counterpart.[5] A key objective of nanocatalysis research is to produce a catalyst with 100% selectivity, extremely high activity, and long lifetime.[5] To this end, the great challenge in constructing

Broader context

The search for effective hydrogen-storage materials remains one of the most challenging barriers in the implementation of a "hydrogen economy" society. Hydrazine monohydrate is considered as a promising hydrogen storage material because of its high hydrogen content, easy recharging as a liquid employing the current infrastructure for liquid fuels, and only producing nitrogen in addition to hydrogen, which does not need on-board collection for recycling. However, to enable hydrazine monohydrate for practical hydrogen storage, one must avoid the undesired reaction pathway to ammonia. Herein, graphene is first employed and proved to be a powerful dispersion agent and distinct support for the RhNi nanoparticles, and unexpectedly, the resultant catalyst exerts 100% H_2 selectivity, excellent activity and stability toward complete decomposition of hydrous hydrazine under ambient conditions, thanks to the great role of graphene as a communicating platform in facilitating the electron transfer and mass transport kinetics during the catalytic reaction process. These encouraging results would certainly assist endeavors to further enhance the terribly sluggish catalytic kinetics of hydrazine monohydrate decomposition catalyst. The utilization of graphene as a catalyst support would lead to next-generation catalysts and herald significant changes in the economy and environmental impact of chemical production.

a nanocatalyst is to develop a large area of carbon surface which must ensure the catalyst particles disperse without any aggregation and be capable of facilitating the electron transfer and mass transport kinetics during the catalytic reaction process.[5d-g]

Graphene,[6] as a single-atom-thick carbon material,[6a] inherently holds many advantages such as extremely high surface area,[6b-c] fantastic thermal/electrical conductivity,[6d-e] light weight, excellent flexibility and mechanical strength,[6f-i] *etc.*, and thus is expected to find exciting applications in electronics, engineering materials as well as an ideal substrate for high-performance catalysts. Although many studies have been focused on graphene-based materials for microelectronics, composite reinforcement, supercapacitor, lithium-ion battery, and so on,[7] direct growth and anchoring of functional nanomaterials as catalytically-active components on graphene and then harvesting its catalytic performance has been rarely reported. Thus, boosting the unique role of graphene for catalyst synthesis and activity and comparing with other conventional carbon supports are of great interest.

Herein, graphene-supported RhNi catalyst is successfully synthesized by a facile co-reduction route, wherein the graphene plays a key role as a powerful dispersion agent and distinct support for the RhNi nanoparticles (NPs). Unexpectedly the resultant catalyst exerts 100% H_2 selectivity and exceedingly high activity toward complete decomposition of hydrous hydrazine under ambient conditions. In addition, sodium hydroxide (NaOH) can obviously promote the reaction as well.

The RhNi NPs supported on graphene were synthesized by co-reduction of rhodium(III) chloride and nickel(II) chloride in the presence of graphene oxide (GO) sheets using sodium borohydride as a reducing agent. Then, hydrous hydrazine was introduced into the reaction flask to be catalytically decomposed. The gas generated was identified by mass spectrometry and its amount was measured volumetrically.

Surprisingly, the RhNi catalyst prepared in the presence of GO and NaOH exhibits 100% H_2 selectivity [$n(N_2 + H_2)/nN_2H_4 = 3.0$] and remarkably high activity to complete the decomposition reaction of hydrous hydrazine within only 49 min [trace (a), Fig. 1A] at room temperature, which is much faster (as high as 327%) than that of the most active catalysts ever reported for this reaction.[4] The reaction selectivity and completeness are further determined by mass spectrometry (no NH_3 and $H_2/N_2 = 2.0$, Fig. 1B) and ultraviolet visible (UV-Vis) spectra (no N_2H_4 after reaction, Fig. S1†), respectively. On the contrary, for the RhNi catalyst prepared without GO and NaOH, only 1.4 equiv of gases (H_2 selectivity: 40%) can be released from hydrous hydrazine even after more than 19 h [trace (b), Fig. 1A], which is more than 23 times worse than that of RhNi catalyst prepared with GO and NaOH.

The inductively coupled plasma atomic emission spectroscopy (ICP-AES) results show that the Rh/Ni ratio of catalysts prepared with and without GO sheets are 4.69 and 4.62, respectively, which are almost in agreement with the ratio of metal precursors. The relative change in the D to G peak intensity ratio before and after the reduction in the Raman spectra (Fig. 2A) confirms the reduction of GO during the preparation of the RhNi NPs.[8] We then analyzed the X-ray diffraction patterns (XRD) of the two kinds of catalysts, attempting to determine the underlying causes for their distinct catalytic activities. Interestingly, it clearly shows that the diffraction peaks of RhNi NPs supported on graphene are much weaker than that of RhNi NPs without graphene support (Fig. 2B), indicating that graphene can effectively restrain the growth of RhNi NPs. The prominent diffraction peaks are similar to Rh, which might be due to the relatively low content of Ni. The microstructures of the two samples are then characterized by scanning electron microscopy (SEM) and transmission electron microscopy (TEM) (Fig. 3). As can be seen from Fig. 3a and 3b, the RhNi NPs prepared with GO are well dispersed on graphene with an average particle size of ~5 nm (Fig. S2A†). On the contrary, the RhNi NPs prepared without GO (Fig. 3c and 3d) are severely aggregated to much larger particles (*ca.* 26 nm, Fig. S2B†). This is consistent with the XRD results. The smaller size and lack of agglomeration indicate that GO can successfully serve as not only a support but also an efficient dispersing agent for the synthesis of RhNi NPs in aqueous solution, which is understandable because the hydrophobic basal plane and the hydrophilic phenyl epoxide and hydroxyl groups endow GO with the ability as a surfactant,[9] which can anchor RhNi NPs and thus control its size and distribution on the graphene during the synthetic process. In addition, the high resolution TEM images (Fig. S3a and 3b†) and the corresponding selected area energy dispersion (SAED) patterns (Fig. 3b and 3d inset) indicate that both catalysts are in a polycrystalline state. Energy-dispersive X-ray spectroscopy (EDS) shows that Rh and Ni are the main components of the catalysts (Fig. S3c and 3d†). Elemental mapping profiles of Rh and Ni indicate the formation of homogenous alloy NPs prepared *via* co-reduction method (Fig. S4†).

As a unique form of carbon, graphene has capabilities that make it superior to other kinds of carbon as support for catalyst. For comparison, we synthesized RhNi NPs supported on the state-of-the-art carbon support (Vulcan XC-72R). To our surprise, although they

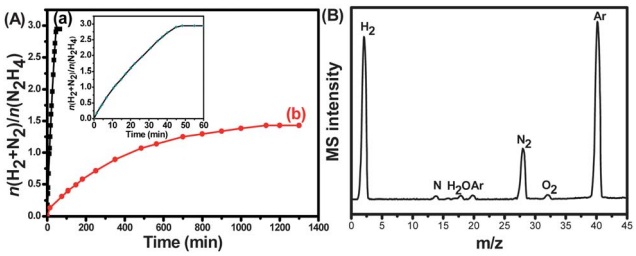

Fig. 1 (A) Time profiles for decomposition of hydrazine monohydrate catalyzed by the RhNi NPs prepared (a) with and (b) without NaOH and GO sheets. Inset: the expanded view of (a). (B) Mass spectral (MS) profile of gases released from the complete decomposition of hydrous hydrazine at room temperature.

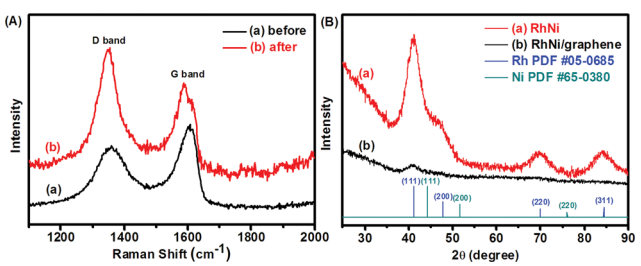

Fig. 2 (A) Raman spectra of GO (a) before and (b) after the reduction. (B) XRD profiles of (a) RhNi NPs supported on graphene and (b) RhNi NPs alone.

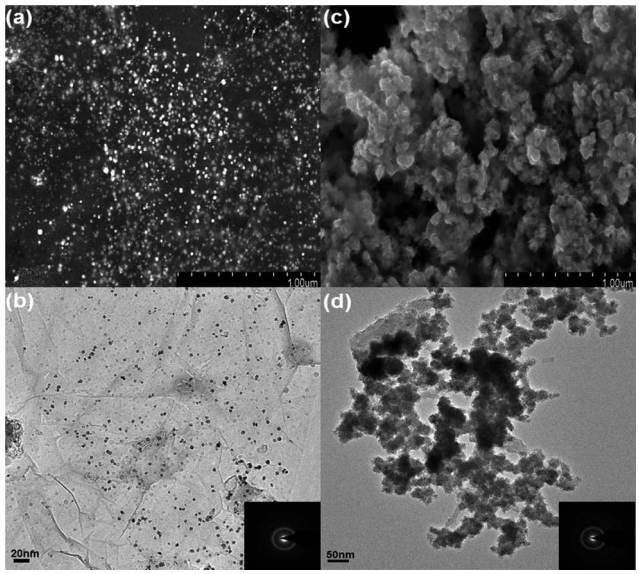

Fig. 3 SEM (a, c) and TEM (b, d) images of RhNi NPs prepared (left) with and (right) without GO sheets and NaOH. The insets in (b) and (d): the corresponding SAED pattern.

had similar size, distribution and crystal structure (SEM and TEM in Fig. S5; XRD profile in Fig. S6†), the activity of RhNi NPs grown on XC-72R is much lower than that with graphene (Fig. S7†), highlighting the synergistic effect of graphene and active component NPs, stemming from the intimate interactions and consequently efficient electron transfer and/or mass transport between the active component NPs and the conductive single-atom-thick 2-D graphene network.[10]

The above mentioned results indicate that the excellent activity of RhNi NPs supported on graphene can be reasonably attributed to the combined effect of good dispersion and the intimate interaction derived from graphene. However, we need to also consider whether NaOH can also affect the catalyst performance as well. To this end, the NaOH present in the synthesis process of RhNi/graphene is washed away and then its catalytic performance tested. The result shows that the selectivity and activity of the catalyst decrease significantly (only 1.42 equiv of gases released even after 900 min) (Fig. S8a†). Interestingly, this degenerative performance can be recovered when an equivalent amount of NaOH is subsequently re-added to the reaction flask, indicating that NaOH indeed affects the selectivity and activity of the decomposition of hydrous hydrazine (Fig. S8b†). Similarly, the addition of NaOH can also obviously improve the catalytic performance of RhNi NPs synthesized without GO and NaOH (Fig. S9†), further confirming the effect of NaOH. However, this enhanced catalytic performance (Fig. S9b†) is still inferior to that of RhNi with graphene (Fig. S8b†), highlighting the role of graphene again.

The fact that hydrous hydrazine is very stable in the solution of GO and NaOH indicates that NaOH only serves as a catalyst promoter, not a catalyst, for the reaction (Fig. S10†). This is understandable because the existence of OH^- could decrease the concentration of undesirable $N_2H_5^+$ ($N_2H_5^+ + OH^- \rightleftharpoons N_2H_4 + H_2O$) in aqueous solution[11] and also promote the rate-determining deprotonation step ($N_2H_4 \rightarrow N_2H_3^* + H^*$) along the decomposition process of N_2H_4 to N_2 and H_2.[12] Besides promoting the reaction kinetics, the alkaline solution helps to inhibit the formation of NH_3 and thereby obtain 100% H_2 selectivity.[4g] In addition, the similarity in catalytic performance of RhNi NPs with KOH or NaOH indicates that the alkaline promotion role is general instead of alkali type-dependent (Fig. S11†).

To determine the effect of the amount of NaOH on the catalytic performance, graphene supported RhNi catalysts are prepared with various amounts of NaOH. It is found that the selectivity and activity of catalysts for the decomposition of hydrous hydrazine increase with the amount of NaOH until the amount reaches 2 mL, after which further increase in the amount of NaOH has almost no effect on the decomposition of hydrous hydrazine (Fig. S12†).

As for the stability of the RhNi/graphene catalyst, we successively test its catalytic performance by adding aliquots of hydrazine monohydrate into the reaction vessel after the completion of the previous run. The result shows no significant catalytic activity decrease over 3 cycles (Fig. S13†).

In summary, we have found a facile method to synthesize well-dispersed RhNi NPs grown on graphene. The graphene proved to be a distinct and powerful support for the RhNi-based catalyst. Surprisingly, the resultant RhNi@graphene catalyst exerts excellent catalytic performance for the decomposition of hydrous hydrazine at room temperature, wherein NaOH plays a great role as a promoter as well. The obtained catalyst is believed to open new and exciting possibilities to promote the practical application of hydrous hydrazine for chemical hydrogen storage. The utilization of graphene as a two-dimensional support to anchor active component NPs and to facilitate the electron transfer and mass transport kinetics opens up new avenues for designing next generation catalysts.

Acknowledgements

This work is financially supported by 100 Talents Programme of The Chinese Academy of Sciences, National Natural Science Foundation of China (Grant No. 21101147), and the Jilin Province Science and Technology Development Program (Grant No. 20100102 and 20116008). The authors thank Professor Qiang Xu for helpful discussions. The authors also acknowledge Lei Wang, Guohui Chang and Wenbo Lu for help with Raman and UV-Vis experiments.

Notes and references

1 (*a*) L. Schlapbach and A. Zuttel, *Nature*, 2001, **414**, 353; (*b*) P. Chen, Z. Xiong, J. Luo, J. Lin and K. L. Tan, *Nature*, 2002, **420**, 302; (*c*) W. Grochala and P. P. Edwards, *Chem. Rev.*, 2004, **104**, 1283; (*d*) J. M. Ogden, *Annu. Rev. Energy Environ.*, 1999, **24**, 227.

2 (*a*) J. Graetz, *Chem. Soc. Rev.*, 2009, **38**, 73; (*b*) N. L. Rosi, J. Eckert, M. Eddaoudi, D. T. Vodak, J. Kim, M. O'Keeffe and O. M. Yaghi, *Science*, 2003, **300**, 1127; (*c*) C. W. Hamilton, R. T. Baker, A. Staubitz and I. Manners, *Chem. Soc. Rev.*, 2009, **38**, 279; (*d*) A. Gutowska, L. Li, Y. Shin, C. M. Wang, X. S. Li, J. C. Linehan, R. S. Smith, B. D. Kay, B. Schmid, W. Shaw, M. Gutowski and T. Autrey, *Angew. Chem., Int. Ed.*, 2005, **44**, 3578; (*e*) H. L. Jiang, S. K. Singh, J. M. Yan, X. B. Zhang and Q. Xu, *ChemSusChem*, 2010, **3**, 541; (*f*) T. He, H. Wu, G. Wu, J. Wang, W. Zhou, Z. Xiong, J. Chen, T. Zhang and P. Chen, *Energy Environ. Sci.*, 2012, **5**, 5686.

3 (*a*) E. W. Schmidt, *Hydrazine and its Derivatives: Preparation, Properties, Applications*, 2nd ed.; John Wiley & Sons: New York, 1984; (*b*) S. J. Cho, J. Lee, Y. S. Lee and D. P. Kim, *Catal. Lett.*, 2006, **109**, 181; (*c*) M. Zheng, R. Cheng, X. Chen, N. Li, L. Li, X. Wang and T. Zhang, *Int. J. Hydrogen Energy*, 2005, **30**, 1081; (*d*) W. E. Armstrong, L. B. Ryland, H. H. Voge, U.S. Patent 4,124,538, 1978; (*e*) M. Zheng, X. Chen, R. Cheng, N. Li, J. Sun,

X. Wang and T. Zhang, *Catal. Commun.*, 2006, **7**, 187; (*f*) X. Chen, T. Zhang, M. Zheng, Z. Wu, W. Wu and C. Li, *J. Catal.*, 2004, **224**, 473; (*g*) Y. Nakajima, A. Inagaki and H. Suzuki, *Organometallics*, 2004, **23**, 4040; (*h*) J. B. O. Santos, G. P. Valença and J. A. J. Rodrigues, *J. Catal.*, 2002, **210**, 1, and references therein; (*i*) R. R. Schrock, T. E. Glassman, M. G. Vale and M. Kol, *J. Am. Chem. Soc.*, 1993, **115**, 1760; (*j*) H. Gu, R. Ran, W. Zhou, Z. Shao, W. Jin, N. Xu and J. Ahn, *J. Power Sources*, 2008, **177**, 323; (*k*) J. Prasad and J. L. Gland, *Langmuir*, 1991, **7**, 722.

4 (*a*) S. H. Wu and D. H. Chen, *J. Colloid Interface Sci.*, 2003, **259**, 282; (*b*) S. K. Singh, X. B. Zhang and Q. Xu, *J. Am. Chem. Soc.*, 2009, **131**, 9894; (*c*) S. K. Singh and Q. Xu, *J. Am. Chem. Soc.*, 2009, **131**, 18032; (*d*) D. G. Tong, X. L. Zeng, W. Chu, D. Wang and P. Wu, *Mater. Res. Bull.*, 2010, **45**, 442; (*e*) S. K. Singh and Q. Xu, *Inorg. Chem.*, 2010, **49**, 6148; (*f*) S. K. Singh and Q. Xu, *Chem. Commun.*, 2010, **46**, 6545; (*g*) S. K. Singh, A. K. Singh, K. Aranishi and Q. Xu, *J. Am. Chem. Soc.*, 2011, **133**, 19638.

5 (*a*) R. Ferrando, J. Jellinek and R. L. Johnston, *Chem. Rev.*, 2008, **108**, 845; (*b*) C. T. Campbell, S. C. Parker and D. E. Starr, *Science*, 2002, **298**, 811; (*c*) Y. Xia, Y. Xiong, B. Lim and S. E. Skarabalak, *Angew. Chem., Int. Ed.*, 2009, **48**, 60; (*d*) B. Fang, N. K. Chaudhari, M. S. Kim, J. H. Kim and J. S. Yu, *J. Am. Chem. Soc.*, 2009, **131**, 15330; (*e*) D. Eder, *Chem. Rev.*, 2010, **110**, 1348; (*f*) A. I. Hochbaum and P. Yang, *Chem. Rev.*, 2009, **110**, 527; (*g*) J. A. Martinez, N. Misra, Y. Wang, C. Grigoropoulos, P. Stroeve and A. Noy, *Nano Lett.*, 2009, **9**, 1121; (*h*) J. Li, H. Fan and X. Jia, *J. Phys. Chem. C*, 2010, **114**, 14684.

6 (*a*) A. K. Geim and K. S. Novoselov, *Nat. Mater.*, 2007, **6**, 183; (*b*) X. Li, X. Wang, L. Zhang, S. Lee and H. Dai, *Science*, 2008, **319**, 1229; (*c*) M. D. Stoller, S. J. Park, Y. W. Zhu, J. H. An and R. S. Ruoff, *Nano Lett.*, 2008, **8**, 3498; (*d*) A. A. Balandin, S. Ghosh, W. Z. Bao, I. Calizo, D. Teweldebrhan, F. Miao and C. N. Lau, *Nano Lett.*, 2008, **8**, 902; (*e*) K. S. Novoselov, A. K. Geim, S. V. Morozov, D. Jiang, M. I. Katsnelson, I. V. Grigorieva, S. V. Dubonos and A. A. Firsov, *Nature*, 2005, **438**, 197; (*f*) A. Fasolino, J. H. Los and M. I. Katsnelson, *Nat. Mater.*, 2007, **6**, 858; (*g*) C. Lee, X. D. Wei, J. W. Kysar, and J. Hone, *Science*, 2008, **321**, 385; (*h*) X. Huang, X. Qi, F. Boey and H. Zhang, *Chem. Soc. Rev.*, 2012, **41**, 666; (*i*) X. Huang, Z. Y. Yin, S. X. Wu, X. Y. Qi, Q. Y. He, Q. C. Zhang, Q. Y. Yan, F. Boey and H. Zhang, *Small*, 2011, **7**, 1876.

7 (*a*) K. S. Novoselov, D. Jiang, F. Schedin, T. J. Booth, V. V. Khotkevich, S. V. Morozov and A. K. Geim, *Proc. Natl. Acad. Sci. U. S. A.*, 2005, **102**, 10451; (*b*) S. Stankovich, D. A. Dikin, G. H. B. Dommett, K. M. Kohlhaas, E. J. Zimney, E. A. Stach, R. D. Piner, S. T. Nguyen and R. S. Ruoff, *Nature*, 2006, **442**, 282; (*c*) K. Zhang, L. L. Zhang, X. S. Zhao and J. Wu, *Chem. Mater.*, 2010, **22**, 1392; (*d*) J. K. Lee, K. B. Smith, C. M. Hayner and H. H. Kung, *Chem. Commun.*, 2010, **46**, 2025; (*e*) X. Cao, Y. Shi, W. Shi, G. Lu, X. Huang, Q. Yan, Q. Zhang and H. Zhang, *Small*, 2011, **7**, 3163; (*f*) J. Liu, Z. Yin, X. Cao, F. Zhao, A. Ling, L. Xie, Q. Fan, F. Boey, H. Zhang and W. Huang, *ACS Nano*, 2010, **4**, 3987; (*g*) B. Li, X. Cao, H. G. Ong, J. W. Cheah, X. Zhou, Z. Yin, H. Li, J. Wang, F. Boey, W. Huang and H. Zhang, *Adv. Mater.*, 2010, **22**, 3058; (*h*) Q. He, S. Wu, S. Gao, X. Cao, Z. Yin, H. Li, P. Chen and H. Zhang, *ACS Nano*, 2011, **5**, 5038; (*i*) Q. He, H. G. Sudibya, Z. Yin, S. Wu, H. Li, F. Boey, W. Huang, P. Chen and H. Zhang, *ACS Nano*, 2010, **4**, 3201; (*j*) Y. Sun, Q. Wu and G. Shi, *Energy Environ. Sci.*, 2011, **4**, 1113.

8 S. Stankovich, D. A. Dikin, R. D. Piner, K. A. Kohlhaas, A. Kleinhammes, Y. Jia, Y. Wu, S. T. Nguyen and R. S. Ruoff, *Carbon*, 2007, **45**, 1558.

9 (*a*) J. Kim, L. J. Cote, F. Kim, W. Yuan, K. R. Shull and J. Huang, *J. Am. Chem. Soc.*, 2010, **132**, 8180; (*b*) K. Jasuja and V. Berry, *ACS Nano*, 2009, **3**, 2358.

10 (*a*) W. Qin and X. Li, *J. Phys. Chem. C*, 2010, **114**, 19009; (*b*) S. Sharma, A. Ganguly, P. Papakonstantinou, X. Miao, M. Li, J. L. Hutchison, M. Delichatsios and S. Ukleja, *J. Phys. Chem. C*, 2010, **114**, 19459.

11 K. Yamada, K. Asazawa, K. Yasuda, T. Ioroi, H. Tanaka, Y. Miyazaki and T. Kobayashi, *J. Power Sources*, 2003, **115**, 236.

12 V. Rosca, M. Duca, M. T. Groot and M. T. M. Koper, *Chem. Rev.*, 2009, **109**, 220.

